

Seismic Tomography on the near vertical incidence reflection data from Ionian Sea¹

Eleni. Kokinou², Antonios. Vafidis², Ioannis F. Louis³

² Applied Geophysics Lab. Dep. of Mineral Resource Eng. Technical Univ. of Crete, Chania, Greece 73100. :

ekokinou@mred.tuc.gr; vafidis@mred.tuc.gr

³ Department of Geophysics & Geothermic, University of Athens, Panepistimiopolis, Ilissia, Athens 15784, Greece.

jlouis@geol.uoa.gr; flouis@geol.uoa.gr

Abstract: *A part of deep reflection data from Ionian Sea carried out in 1992 has been processed in order to improve their quality. Combination of well – known filters has been applied in our attempt to increase the signal to noise ratio of the data. Reflections have been detected and picked by studying the shot gathers. Thereinafter the reflection times and offsets were used in order to reveal the 2-D reflection tomography of the study area. The velocity model of the area produced by analyzing the data is compared with the tomographic model. Then the migrated section of the study area is interpreted by combined the results from the seismic tomography and the standard seismic processing with geologic and drilling data.*

Keywords: Hellenic arc, Pre – Apulian zone, filtering, reflection tomography.

INTRODUCTION

Seismic tomography means a picture of the earth structure based on seismic velocities. The possibility of exploiting different wave types jointly and an arbitrary distribution of sources and receivers comprise an important advantage of the seismic tomography over other inversion methods (Vesnaver, 1996). Reflection tomography comprises an inversion method using the travel times of reflected waves and offsets to determine the seismic velocities and the subsurface structure (Neumann, 1981; Rappin, 1987). Reflection tomography under specific conditions (Ivansson, 1986) gives the best seismic velocity determination in comparison with the conventional seismic methods (Bishop et al., 1985).

Dyer and Worthington (1988) developed an iterative 2-D reflection tomography method, while Carrion and Bohm (1994) proposed the simulated annealing method. Vesnaver (1996) show the contribution of reflected, refracted and transmitted waves to seismic tomography. The possibility to invert 2- D and 3-D travel time data and to obtain accurate information about the subsurface structure has been already shown (Carrion et al., 1993b; Boehm et al., 1996, 1997). Schmid at al. (2001) investigated the eastern Dabie Shan in China in order to study the crustal structure of the area by applying reflection seismic and tomographic inversion techniques. Lutter et al. (1994) inverted high resolution seismic data to provide the first reliable images of internal details of the Columbia River Basalt Group (CRBG), the subsurface basalt /sediment interface and the deeper sediment/basement interface. The technique used to invert first arrivals travel times incorporates a splined velocity parameterization and a rapid procedure for calculating partial derivatives necessary for gradient methods. The partial derivatives of travel time with respect to velocity are calculated by velocity node perturbation using Fermat's principle.

¹ Journal of the Balkan Geophysical Society (In Press)

The inversion of large – offset reflection times (wide – angle reflection data) has been also used for the velocity determination (Bortfeld, 1957; Kaila and Krishna, 1979). Al – Chalabi (1974) pointed out that the velocity estimation from large – offset reflection times by hyperbolic approximation causes large errors in the determination of interval velocity unless an appropriate adjustment for refraction effects is allowed. Le Pichon et al. (1968) determined the velocity model for deep – sea sediments by recording both wide – angle and low – angle reflection data. Sain and Kaila (1994) used the damped least squares for the inversion of wide - angle seismic reflection times.

In the present study we improved the data quality and picked the reflection times in shot gathers. The CAT3D tomographic packet was used for the inversion of the reflection times. Thereinafter, the stacked and migrated sections of the study area were produced. The velocity models revealed by the reflection tomography and the velocity analysis are compared in order to validate the tomographic model. Finally we interpret the migrated section using the velocity model of the area in combination with geologic and drilling data.

SEISMIC TOMOGRAPHY PROCEDURE

Reflection tomography estimates the velocity field of the study area usually based on reflection times of near vertical incidence data. It is usually assumed that the medium composes of a finite number of elements, each of which has a discrete value of the velocity. The first step for the reflection tomography is the picking of P – waves travel times in CDP gathers. The velocity and interface functions in the seismic model are polynomial (Phadke and Kanasewich, 1990) with splines functions (Gjoystdal and Ursin, 1981; Gjoystdal et al., 1984) or Fourier series (Chiu and Steward, 1987). Thereinafter the reflection times are computed by using the Ray Tracing theory or the Wave Theory. Three ray tracing techniques are wide known: the Shooting technique, the Bending technique and the Continuation technique. The last step is the inversion of reflection travel times. The equations determined in the previous step are solved and the interval velocity for each earth layer is determined. The inversion starts with an initial guess for the velocity field and reflectors structure. Comparing the experimental travel times with those simulated by the ray tracing or wave algorithm a reflection point is estimated for each reflected arrival. After this the velocity field and the reflector structure is updated.

In the present case we used the reflection times and an offset revealed from the shot gathers. The seismic tomography performed by using the tomographic package CAT3D (Vesnaver, Bohm and Rossi, 1997). The approach adopted here is a 3 - D generalization of that introduced in 2 – D by Carrion et al., (1993 a, b) and later described by Boehm et al., (1996). The macro - model of the velocity field in depth, generated by CAT3D, simulates complex geological structures characterized by lateral velocity anomalies and rugged interfaces. The initial solid velocity model was further processed to generate a more detailed complex model utilizing the PIXEL module of CAT3D. The space is discretized by voxels. These are homogeneous domains with vertical sides, which are planes whose projection on a horizontal plane is a convex polygon. Their horizontal sides coincide with two adjacent geological interfaces, defined by bi-cubic splines. The parameters describing the reflecting interfaces and those describing the velocity field were computed separately and the reason is that in reflection tomography the calculation

of the additional parameters describing the reflecting interfaces, interfere with those describing the velocity field.

The inversion starts with an initial guess for the velocity field and reflectors structure. A reflection point is estimated for each reflected arrival by comparing the experimental travel times with those simulated by a minimum time ray tracing algorithm. After this the velocity field and the reflector structure is updated by imposing that the dispersion of the estimated reflection points is minimum. In the most common approach of tomographic inversion, the investigated area is discretized by voxels, i.e. parallelepipeds where the physical properties are supposed constant in space. Usually the voxel shape and size is the same everywhere, and so the velocity field is estimated in a regular grid. This choice is due to the much simpler software setting up of the tomographic inversion but may lead to serious draw backs. By adopting irregular grids in sequence, the local resolution was matched to one that can be supported by the ray path's distribution. The result is a reliable solution which is not affected by the instabilities.

THE SEISMIC EXPERIMENT

The seismic profiling of the present study was carried out in 1992 with the support of the European Union within the frameworks of the JOULE PROJECT STREAMERS, in order to obtain information about the structure of the crust in Ionian basin. Seven seismic lines (Fig. 1a) of total length 700 Km were scanned in the central Mediterranean Sea. One of these lines namely ION – 7 crosses the deep Ionian basin up to the gulf of Patras.

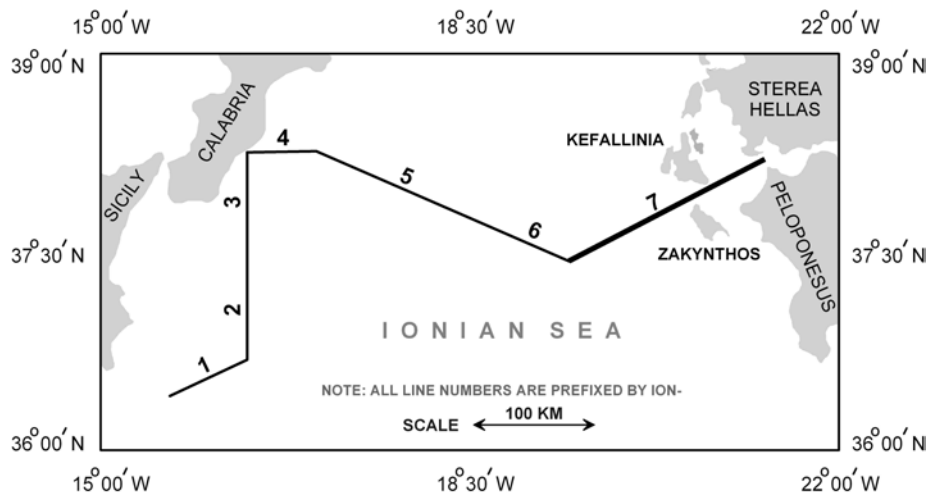


Figure 1 (a) Map of STREAMERS – lines.

The seismic data were recorded by Geco-Prakla's M/V Bin Hai 511 which towed a 36 – airgun tuned array with a capacity of 7118 inch³ (about 120l) (McBride et al., 1994). A 180 channel streamer array produced a 30-fold normal incidence reflection profile. The shot interval was 75 m, the receiver interval 25 m, the minimum offset 180 m, and the sampling interval 4 ms. PROMAX 2D was used for the seismic processing.

Nicolich et al. (1994) presented the results deduced by processing the reflection data from the lines ION – 1 to ION - 6. The most interested conclusion was the detection of a deep crustal layer thick to 1 – 1.5 s TWT (two – way traveltime), corresponding to a wide (3.5 – 4 Km thick) laminated lower crust or crust – mantle transition which suggest an interval velocity of 6.9 – 7.1 Km/s. Hirn et al. (1996) interpreted the seismic profiling of the line ION – 7 in combination with wide angle seismics. A major reflector at a depth of about 13 Km is detected, possibly representing the lower limit of western Hellenides, while the seismic image of disruptions of the Mesozoic sequence suggests a more westerly position for the Ionian thrust than previously assumed. Kamberis et al. (1996) interpreted the eastern part of the line ION – 7, suggesting diapiric movements of Triassic evaporites. The reflector at a depth of about 6 – 7 Km corresponds to Triassic evaporites and is interpreted as the “decollement surface” of the folded belt within the Triassic layer.

The Tyrrhenian - Apennine system is controlled by the west - dipping subduction of the Adria – Ionian lithosphere and by the near north - south convergence between the African and Eurasian plates. Positive values of horizontal velocity denote an eastward motion. The Ionian basin comprises a deep sedimentary basin including Mesozoic to Tertiary sequences (Dercourt et al., 1986) in the eastern wedge of the Mediterranean Ridge (Finetti, 1982). The area of study belongs to the western part of the fold belt of the external Hellenides, formed during the Tertiary times as a result of the convergence between the Eurasian and Apulian continents, which was initiated at the end of Cretaceous. The Ionian and Pre – Apulian (or Paxos) zones underlie both offshore and onshore portions of the wide area of study. Neogene to Quaternary sediments accumulated in basins situated in the above mentioned zones. The development of these basins was strongly controlled by the westward migration of the orogenic front.

The area of study is located (Fig. 1b) between Zakynthos and Kefallinia and from the geological point of view belongs to the Pre – Apulian zone (or Paxos).

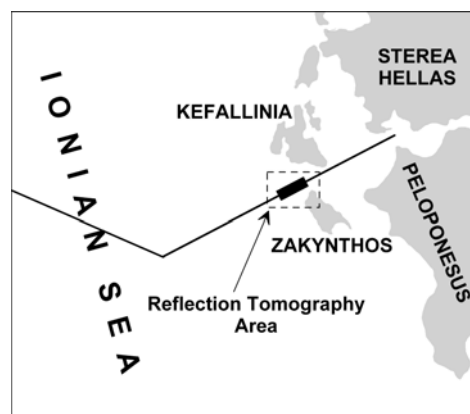


Figure 1 (b) Seismic tomography area.

The Pre – Apulian zone is considered as a transition zone between the Apulian foreland and the Ionian basin. Upper Triassic to Mid. Jurassic sediments include anhydritic/carbonate sequences. The evaporitic sedimentation stopped at the onset of Ionian rifting and pelagic sedimentation represented by limestones interbedded with

cherts and marls. During late Cretaceous to Oligocene, sedimentation occurred in shallow platforms and slope environments. Marlstone sand and shale represent the Miocene, while flysch deposits are unknown in the Pre – Apulian zone.

The reflection data along the seismic line ION-7 exhibit strong sea-bottom and internal multiples from deep and shallow water-bottom, lateral reflections and coherent noise. The above mentioned seismic events imposed difficulties in recognizing the reflections, especially from deeper horizons. Especially, multiples can obscure primary reflections and confuse interpretation of seismic data. In our attempt to increase the signal to noise ratio in the shot gathers used for the seismic tomography we applied various filters and their combinations, such as F – K, noise adaptive filter, deconvolution and bandpass. In the next paragraphs we present the most effective combination of filters, i.e. the F- K, the bandpass and the spiking deconvolution filters.

The F-K filtering is a frequency – wave number filter applied to the data in the frequency – wave number domain (Fail and Grau, 1963; Treitel et al., 1967). F - K analysis allows the display of data in the T – X (conventional time - space) and the F – K (frequency - wave-number) domains, as well as in the F - X and the T - K domains. Data is converted from the time and space sampled traces to the F - K domain by a two dimensional Fourier transform and the polygonal of the accepted signal is designed in the F - K domain. Thereinafter, the F - K filter is applied and the data is converted back by the inverse Fourier transform, so that it is once again in the form of seismic traces. According to F – K analysis for the present data the wave-number k for the multiples ranges between 0 and 0.01 m^{-1} and the frequency F between 10 and 40 Hz. The band-pass filter operates in the frequency domain. One or more sets of the band-pass filter frequencies and a set of the notch filter parameters can be specified. In this case the Butterworth filter was applied. It is a single filter, which was applied to all traces at all times. One group of freq. - slope – freq. -slope needs to be specified. The parameters of the Butterworth filter were 5 - 15 - 20 - 25 until 8000 ms and 5 - 12 - 15 - 20 from 8000 ms until 18000 ms.

The goal of the deconvolution (Yilmaz, 1987) is to compress the wavelet components and eliminate multiples, leaving only the earth's reflectivity in the seismic trace. Spiking deconvolution is the process by which the seismic wavelet is compressed into a zero – lag spike. In the present case minimum phase spiking deconvolution was applied. Proper selection of the spiking deconvolution operator length was accomplished by testing various lengths. The range of the operator length was 80 ms while the pre-whitening was kept at 0.1 %.

Thereinafter shot records were processed using wave equation multiple rejection and deconvolution in order to attenuate the multiple reflections (Kokinou et al. 2002). The RMS – stacking velocities were picked by simultaneously testing the uncorrected gather, the NMO – corrected gather and the velocity spectrum. The RMS velocity model was converted to the interval velocity model using Dix equation. Surface consistent deconvolution has been also applied after stacking to reduce the coherent noise and the lateral reflections. Poststack Kirchhoff migration removed distortions due to lateral velocity variations and improved lateral resolution. The instantaneous attributes associated with the seismic signal computed by Hilbert transform were used in the interpretation of stacked and migrated sections.

RESULTS REVEALED BY PROCESSING THE REFLECTION DATA FROM THE AREA OF STUDY

The combination of F – k, bandpass and spiking deconvolution filters was applied in shot gathers prior the picking of reflection times. Figure 2 presents an example of a filtered shot gather (Fig. 2a) in comparison with the unfiltered shot gather (Fig. 2b).

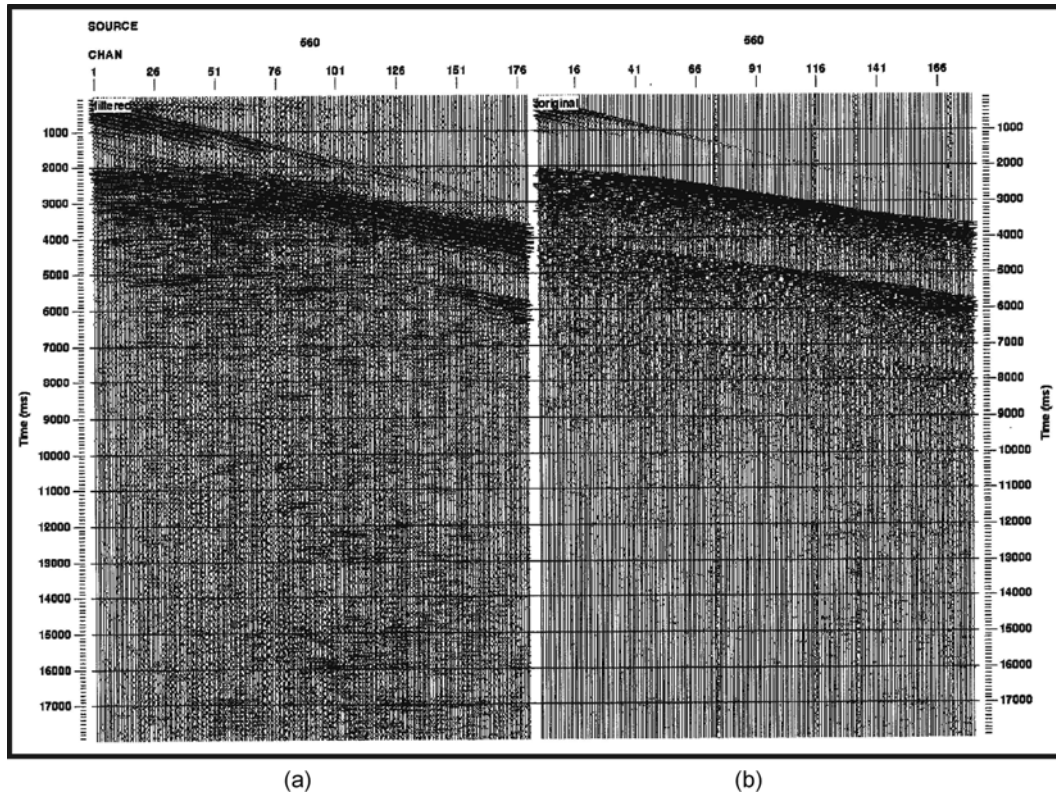


Figure 2 (a) filtered shot gather by F – K, bandpass and spiking deconvolution filters, (b) original shot gather.

The reflections in the filtered shot gather are distinct and continuous, while strong attenuation of the multiple reflections at times greater than 4 s TWT has been maintained. A clear reflection is detected at about 5 s TWT, as well at 12.5 s TWT and at about 17 s TWT.

Figure 3 presents the stacked section of the study area up to 6.5 s TWT, located between 95 and 114 Km of the seismic line ION – 7. The sea bottom is dipping to the west and the sea layer ranges between 1.6 – 0.25 s from the west to the east. Near and parallel to sea - bottom reflectors are possibly present at 2.1 – 0.6 s TWT and at 2.5 – 1 s TWT respectively. A dipping reflector is also detected at 4.5 – 3.2 s TWT, while the presence of a reflector at 5.8 – 5.5 s TWT is very impressive.

Kirchhoff migration was chosen for the data migration because this algorithm offers relative speed and good handling of the vertically variant velocity fields and steep dip handling. Migration involves repositioning data elements to make their locations appropriate to the locations of the associated reflectors or diffracting points. The concept for carrying out Kirchhoff migration (Hagedoorn, 1954; Schneider, 1978) as a

manual operation is to plot a diffraction curve for each depth and slide it along the unmigrated section (keeping the top lined up with zero depth) until a segment of a reflection is tangent to one of the curves.

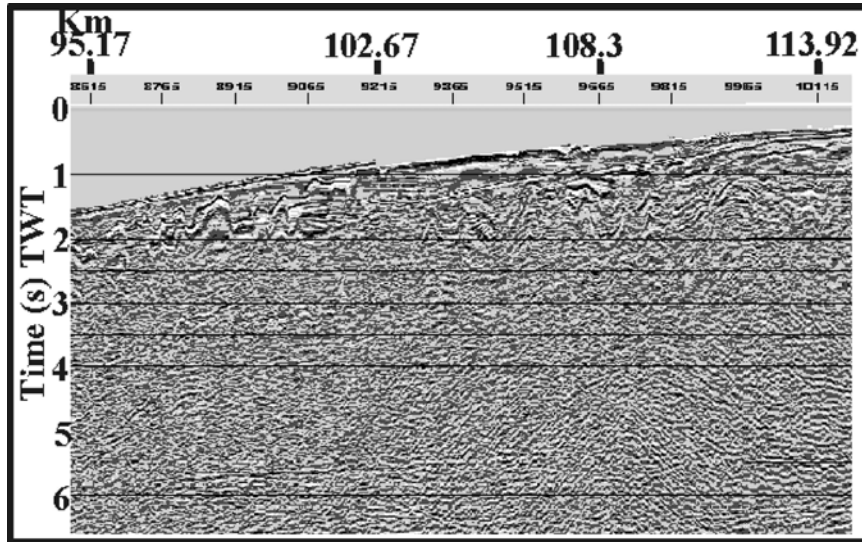


Figure 3 Stacked section of the area located between 95 – 114 Km, v.e = 1:1.

The migration aperture was computed from the data, the maximum dip was 60 ms / trace and the maximum frequency to migrate was 60 Hz. RMS velocities reduced by 20% in order to avoid overmigration were used for Kirchhoff migration. It was applied to the entire stacked section, removed distortions due to lateral velocity variations and improved lateral resolution. Figure (4) presents the migrated section of the study area. A slight overmigration is detected, possibly due to steep lateral velocity variations. The reflectors detected in the stacked section are also present in the migrated section.

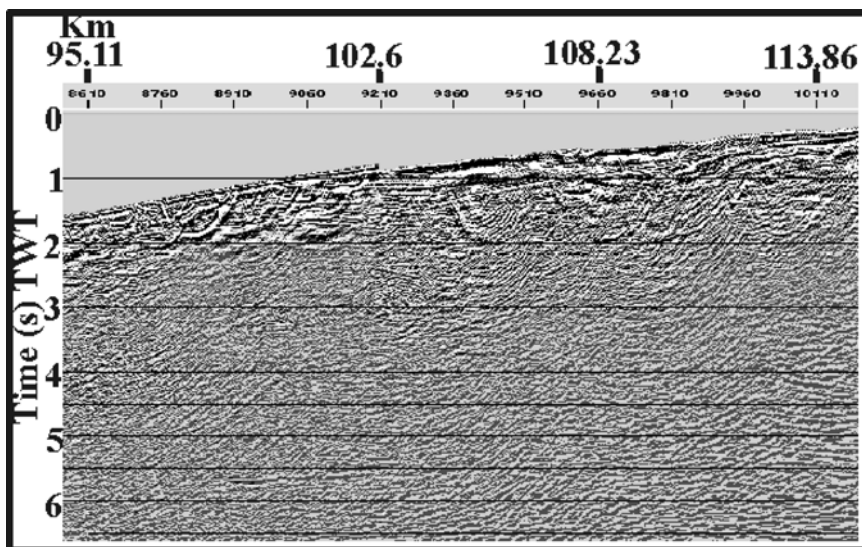


Figure 4 Migrated section of the area located between 95 – 114 Km, v.e = 1:1.

TOMOGRAPHIC AND VELOCITY ANALYSIS MODEL OF THE AREA BETWEEN ZAKYNTHOS AND KEFALLINIA (OFFSHORE)

The study of the filtered shot gathers allow us to pick four reflections, which appeared sufficiently continuous and clear at most offsets. The inversion of the reflection times revealed the tomographic model of the area located between Zakynthos and Kefallinia (Fig. 5) up to 8 Km depth.

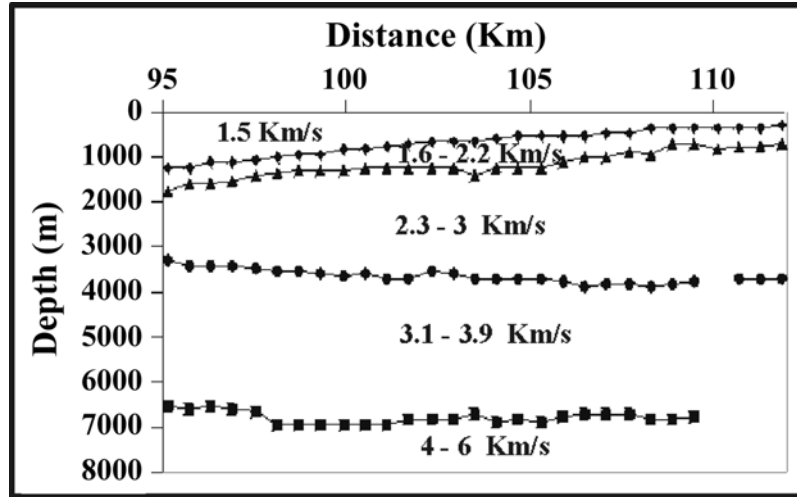


Figure 5 Seismic tomography model up to 8 Km depth of the area located between 95 – 112.5 Km, v.e = 1:1.

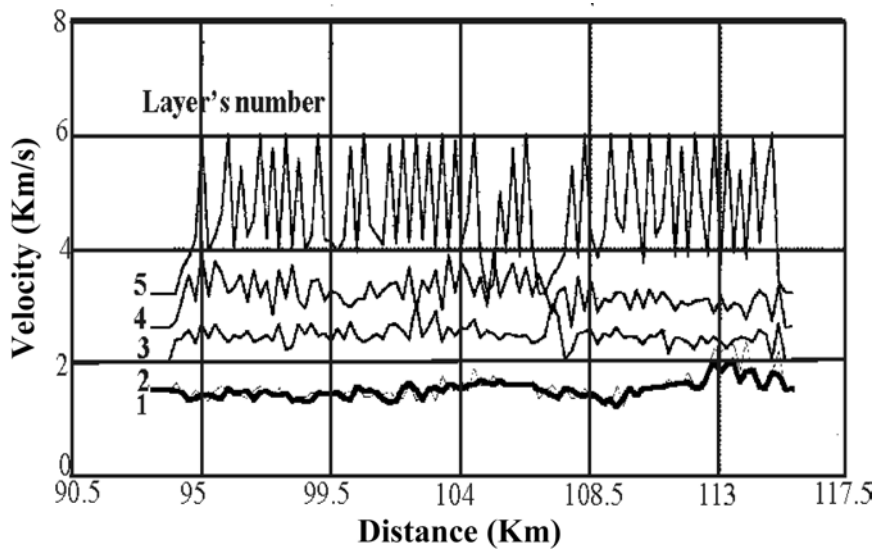


Figure 6 Variation of the velocity for each layer of the tomographic model.

The horizontal axis corresponds to the distance (95 – 112 Km) and the vertical axis to the depth (Km). The first layer corresponds to the sea – layer exhibiting a velocity of about 1.5 Km/s at a depth of about 1.2 – 0.3 Km. The second layer is represented by a velocity of 1.6 – 2.2 Km/s and its bottom is located at a depth of about 1.75 – 0.7 Km. The third layer exhibits a velocity of about 2.3 - 3 Km/s and its bottom is located at a

depth of about 3.7 – 3.3 Km. The following layer is represented by a velocity of about the 3.1 – 3.9 Km/s extended to a depth of about 6.5 – 6.75 Km, underlain by a layer exhibiting a velocity of about 4 – 6 Km/s. An extremely remarkable fact is the velocity ranging in each layer (Fig. 6), that is possibly due to the lateral velocity variations.

Thereinafter, we converted the depth scale of the tomographic model to the time scale, in order to compare both tomographic and velocity analysis model. Figure (7) presents the depth to time conversion of the tomographic model.

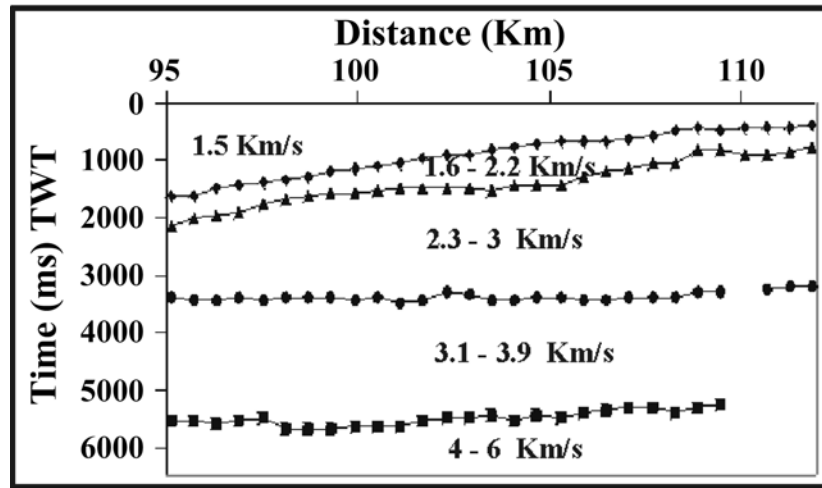


Figure 7 Seismic tomography model in the time scale of the area located between 95 – 112.5 Km, v.e = 1:1.

The sea layer is ranging between 1.6 – 0.4 s TWT and the near to sea – bottom dipping reflectors between 2.2 – 0.8 s TWT and 3.4 – 3.2 s TWT respectively. Finally the last reflector is detected between 5.6 – 5.3 s TWT. Figure 8 presents the distribution of the interval velocities resulted by the velocity analysis of the CDP gathers corresponding to the area of study. In general the velocity model resulted by the velocity analysis seems more complicated in comparison with the tomographic model. Strong lateral velocity variations are also present in the velocity analysis model. We distinguished six layers in the velocity analysis model, instead of five in the tomographic model. The upper layer corresponds to the sea layer exhibiting a velocity of about 1.5 Km/s, ranging between 1.65 – 0.3 s TWT. The first layer under the sea bottom exhibiting a velocity of about 2 – 2.5 Km/s and extended to 2.2 – 0.7 is dipping and parallel to the sea bottom. The approximation of the tomographic and velocity analysis model is good for the first two layers. The next layer of the velocity analysis model corresponding to a velocity of about 2.6 – 3.5 Km/s and ranging between 2.3 – 1.2 s TWT is also dipping, while the respective layer is not detected in the tomographic model. The underlying layer of about 3.6 – 4.5 Km/s with its bottom located at about 3.5 - 2.9 s TWT is also present in the tomographic model but with lower velocity. The last interface is located at 5.8 – 5 s TWT separating two layers of 4.6 – 6 Km/s and >6 Km/s respectively and is also present in the tomographic model.

The area of study is attracting considerable attention due to the complexities of its tectonic setting. The seismic section images a portion of the Hellenic arc consisting of

the Pre – Apulian zone sediments. The presence of thrusts verifies the westward migration of the Hellenic thrust fold. The interpretation of the migrated section (Fig. 7) has been done by combined the tomographic model, the velocity analysis model, geologic and drilling data near to the seismic line.

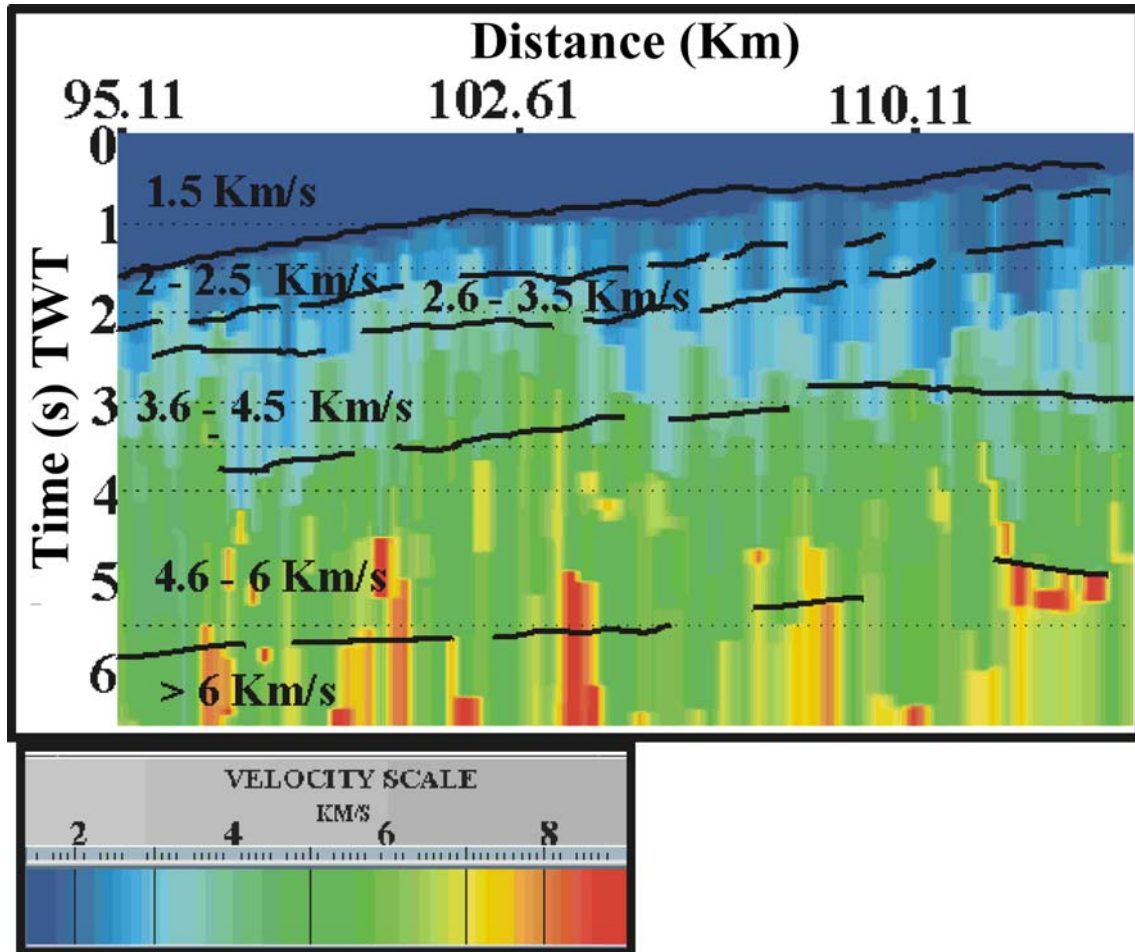


Figure 8 Interval velocity distribution revealed by velocity analysis of the area located between 95 – 114 Km. The velocity ranges between 1.5 – 9 Km/s, v.e = 1:1.

The upper layer corresponds to Plio – Quaternary sediments (P – Q, 2 - 2.5 Km/s) underlain by the Upper Miocene – Lower Pliocene sediments (Mi – Pli, 2.6 – 3.5 Km/s). The next layer represents the Mesozoic carbonates of the Pre – Apulian zone (Px, 3.6 – 4.5 Km/s). Additional stratigraphic control of the previous layers provides the well of South Kefallinia – 1 (SK – 1, Kamberis et al., 1998). In the South Kefallinia – 1 well the following sequences were drilled: (1) Upper Pliocene with fauna of *Gl. Inflata* and *Gl. Crassaformis*; (2) Lower Pliocene with fauna of *Gl. Puncticulata* and *Gl. Margaritae*; (3) Upper Miocene with fauna of *Gl. Conomiozea* and finally (4) Upper Cretaceous carbonates. These sequences are separated by unconformities. The Upper Pliocene - Upper Miocene in the South Kefallinia – 1 well are extended to a depth of about 1.15 Km, while the Plio – Quaternary and Miocene – Lower Pliocene sediments in the migrated section are extended to 1.2 s TWT (about 1.3 Km). The Upper Cretaceous

carbonates in South Kefallinia – 1 well are located between 1.3 – 2.2 Km that is also in agreement with the Mesozoic carbonates found in the migrated section.

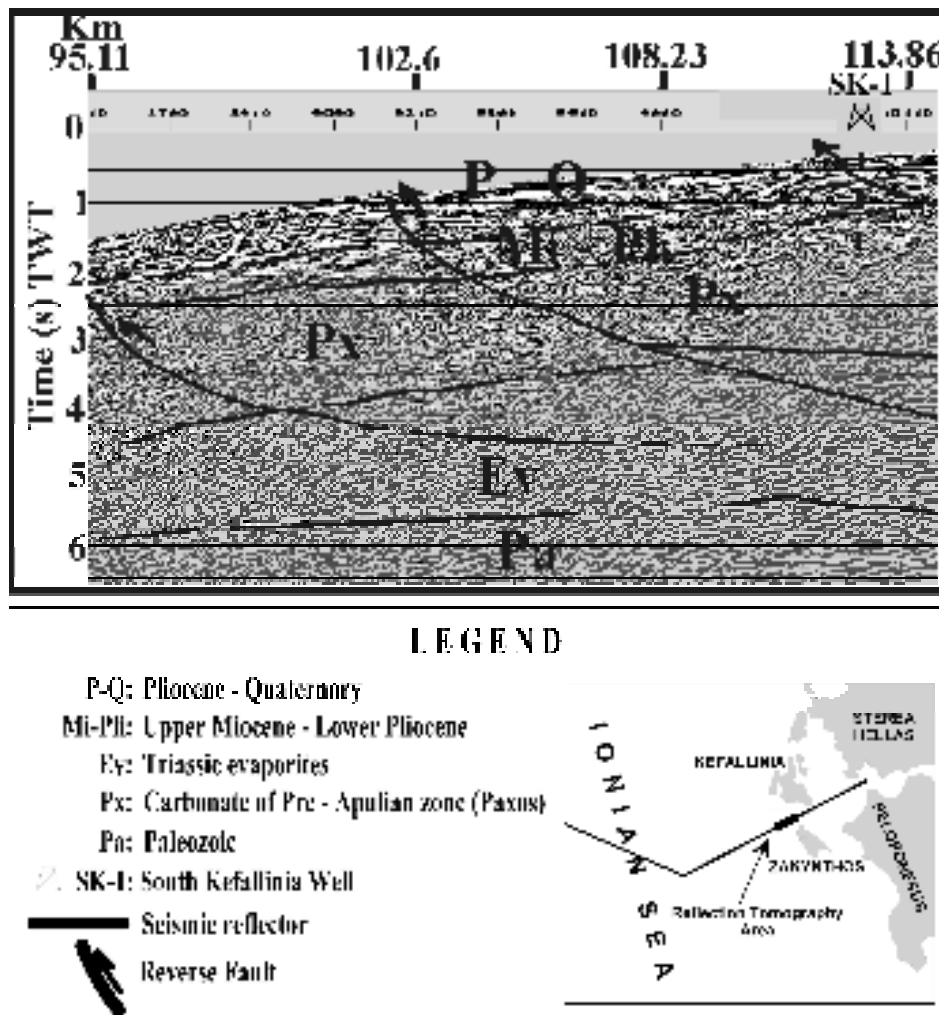


Figure 9 Interpretation of the migrated section located between 95 – 114 Km, v.e = 1:1.

The increased thickness of the Alpine sediments is due to the presence of the Triassic evaporites (Ev, 4.6 – 5.5 Km/s). Large thrusts in Triassic evaporites are present in the area of study. The last layer revealing a velocity of about 5.6 – 6.5 Km/s could represent the Paleozoic sequence (Pa). The existence of the Apulian magnetic basement including Paleozoic sequence is well known in Italy.

CONCLUSIONS

In our attempt to model an area with complex geologic structure we followed two different processes in order to define the interval velocities and thicknesses, i.e. the inversion of reflection times (reflection tomography) and the standard seismic processing. Different prestack techniques were also applied in order to increase the signal to noise ratio during the two processes. The following results are deduced: F – K, bandpass and spiking deconvolution filters were applied in the shot gathers used for the

seismic tomography aiming at reducing the effect of multiple reflections and noise. After the application of the above filters we were able to discriminate the deeper reflections but the relative amplitudes were affected. The effectiveness of prestack filtering in the relative amplitudes during the standard seismic processing was negligible (Kokinou et al. 2002).

In general the tomographic model based on the picking of the reflection times in the shot gathers revealed a general image for the area of study but the detailed model came to light by the velocity analysis of the CDP gathers. The lateral velocity variation is almost the same for both models. The tomographic model approximates well the velocity analysis model for the sea – layer and the underlain layer considering the velocities and the reflection times. The approximation of the two models is also well for the deeper layers considering the reflection times, while the velocities differ of about 0.5 – 1 Km/s.

In concluding the reflection tomography in the present study provides a good macro – model of the velocity field and it is considered a necessary step prior to the standard seismic processing in order to reveal a reliable interpretation for the areas with complexities in geologic setting.

ACKNOWLEDGMENTS

The authors are deeply indebted to HELLENIC PETROLEUM Company (EL.PE) and the University of Athens for the availability of the data. Special thanks are due to the editors and reviewers for the suggestion of the constructive changes in this paper.

REFERENCES

- Al-Chalabi, M., 1974, An analysis of stacking, average, and interval velocities of a horizontally layered ground: *Geophys. Prosp.*, **22**, 458 – 475.
- Bishop, T.N., Bube, K.P., Gutler, R.T., Langan, R.T., Love, P.L., Resnick, J.R., Shuey, R.T., Spindler, D.A., and Wyld, H.W., 1985, Tomographic determination of velocity and depth in laterally varying media: *Geophysics*, **51**, 903 – 923.
- Boehm, G., Rossi, G., and Vesnaver, A., 1996, 3-D reflection tomography by adaptive irregular grids: 59th Ann. Internat. Mtg., Eur. Ass. Exp.Geophys., Expanded abstracts, C056.
- Boehm, G., Rossi, G., and Vesnaver, A., 1997, Adaptive regridding in 3-D reflection tomography: *Annali di Geofisica*, 69 – 83.
- Bortfeld, R., 1957, A method of dip corrections for expanding spread velocity measurements: *Geofisica Pura e Applicata*, **38**, 32 – 44.
- Carrion, P., Boehm, G., Marchetti, A., Pettenati, F., and Vesnaver, A., 1993 a, Reconstruction of lateral gradients from reflection tomography: *Journal of Seismic Exploration*, **2**, 55 – 67.
- Carrion, P., Marchetti, A., Boehm, G., Pettenati, F., and Vesnaver, A., 1993 b, Tomographic processing of Antarctica's data: *First Break*, **11**, 295 – 301.

- Carrion, P., and Boehm, G., 1994, Seismic reflection tomography, via simulated annealing: *The Leading Edge of exploration*, 679 – 682.
- Dercourt, J., Zonenshain, L.P., Ricon ,L.E., Kazmin, V.G., Le Pichon, X., Knipper, A.L., Grandjaquet, C., Sbertshikov, I.M., Geyssant, J., Lepvrier, C., Pechersky, D.H, Boulin, J., Sibuet, J.C., Savostin, L.A., Sorokhtin, O., Westphal, M., Bazhenov, M.L., Lauer, J.P., Biju – Duval, B., 1986, Geological evolution of the Tethys belt from the Atlantic to the Pamirs since the Lias: *Tectonophysics*, **123**, 241 – 315.
- Dyer, B.C., and Worthington, M.H., 1988, Seismic reflection tomography: *First Break*, **6**, 354 – 366.
- Fail, J. P., and Grau, G., 1963, Les filtres en eventail: *Geophysical Prospecting*, **11**, 131 – 63.
- Finetti, I., 1982, Structure stratigraphy and evolution of the central Mediterranean Sea: *Bolletino di Geofisica Teorica ed Applicata*, **15**, 263 – 341.
- Gjoystdal, H., Reinhardsen, J.E., and Ursin, B., 1984, Traveltime and Wavefront curvature calculations in three – dimensional inhomogeneous layered media with curved interfaces: *Geophysics*, **49**, 1466 – 1494.
- Gjoystdal, H., and Ursin, B., 1981, Inversion of reflection times in three dimensions: *Geophysics*, **46**, 972 – 983.
- Hagedoorn, J. G., 1954, A process of seismic reflection interpretation: *Geophysical Prospecting*, **2**, 85 – 127.
- Hirn, A., Sachpazi, M., Siliqi, R., McBride, J., Marnelis, F., Cernobori, L., and STREAMERS – PROFILES group, 1996, A traverse of the Ionian Islands front with coincident normal incidence/ and wide angle seismics: *Tectonophysics*, **264**, 35 –49.
- Ivansson, S., 1986, Seismic borehole tomography – theory and computational methods: *Proc. IEEE*, **74**, 328 – 338, 1166.
- Kaila, K.L., and Krishna, V.G., 1979, A new computerized method for finding effective velocity from reversed reflection travel time data: *Geophysics*, **44**, 1064 – 1076.
- Kamberis, E., Marnelis, F., Loucoyannakis, M., Maltezou, F., Hirn, A., and STREAMERS group, 1996, Structure and deformation of the External Hellenides based on seismic data from offshore Western Greece: *EAGE Special Publication*, **5**, 207 – 214.
- Kamberis, E., Ioakim, Ch., Tsaila – Monopolis, St., Marnelis, F., Sotiropoulos, S., 1998, Geologic and Paleogeographic evolution of Western Greece during the Neogene – Quaternary period in the geodynamic setting of the Hellenic Arc: *Rom. J. Stratigraphy*, **78**, 63 – 73.
- Kokinou E., Vafidis A., 2002, Deep – water multiple suppression on prestack and poststack reflection data from Ionian Sea: submitted to *Geophysical Prospecting*.
- Le Pichon, X., Ewing, J., and Houtz, R.E., 1968, Deep sea sediment velocity determination made while reflection profiling: *J. Geophys. Res.*, **73**, 2597 – 2614.
- Lutter, W.J., Cathings, R.d., and Jarchow, C.M., 1994, An image of the Columbia Plateau from Inversion of high - resolution seismic data: *Geophysics*, **59**, 1278 – 1289.

- McBride, J.H., White, R.S., Henstock, T.J., and Hobbs, R.W., 1994, Complex structure along a Mesozoic sea – floor spreading ridge: BIRPS deep seismic reflection, Cape Verde abyssal plain: *Geophys. J. Int.*, **119**, 453 – 478.
- Neumann, G., 1981, Determination of lateral inhomogeneities in reflection seismics by inversion of traveltimes residuals: *Geoph. Prosp.*, **29**, 161 – 177.
- Nicolich, R., Cernobori, L., Romanelli, M., Petronio, L., 1994, The Ionian Basin and its margins off southern and eastern Calabria: Draft basis of paper for Budapest Proceedings in Tectonophysics presented at EGS Grenoble, April 1994; Deep Seismics Budapest, September 1994; pre – Vienna EEC report, 1- 17.
- Phadke, S. and Kanasevich, E.R., 1990, Seismic tomography to obtain velocity gradients and three dimensional structure and its application to reflection data on Vancouver Island: *Canadian Journal of Earth Science*, **27**, 104 – 116.
- Rappin, D., 1987, Tomographie sismique en milieu heterogene, Report de stage, TOTAL et Universite Louis Paster.
- Sain, K., and Kaila, K.L., 1994, Inversion of wide – angle seismic reflection times with damped least squares: *Geophysics*, **59**, 1735 – 1744.
- Schmid, R., Ryberg, T., Ratschbacher, L., Schulze, A., Franz, L., Oberhuensli, R., and Dong, S., 2001, Crustal structure of the eastern Dabie Shan interpreted from deep reflection and shallow tomographic data: *Tectonophysics*, **333**, I. 3 – 4, 347 – 359.
- Schneider, W., 1978, Integral Formulation for migration in two and three dimensions: *Geophysics*, **43**, 49 – 76.
- Treitel, S., Shanks, J. L., and Frasier, C. W., 1967, Some aspects of fan filtering: *Geophysics*, **32**, 789 – 900.
- Vesnaver, A., Boehm, G., and Rossi, G., 1997, 3D imaging of an hydrocarbons reservoir, Osservatorio Geofisico Sperimentale de Trieste, Italy.
- Vesnaver, A.L., 1996, The contribution of reflected, refracted and transmitted waves to seismic tomography: a tutorial: *First Break*, **14**, 159 – 168.
- Yilmaz, Ozdogan, 1987, Seismic data processing: Society of Exploration Geophysics.